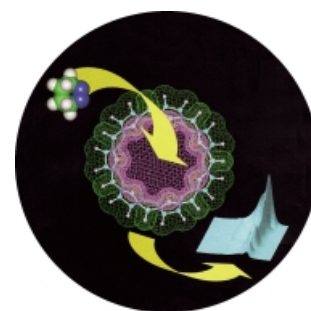


COVER PICTURE

The cover picture shows in the center an electron-density map of the molecular container compound cucurbit[7]uril. The polarizability inside the cavity of this host can be explored through solvatochromic effects on the absorption spectra (bottom right) when probed by the inclusion of an azo chromophore guest (top left). This novel method allows insight into the inner phase of supermolecules. More details about this process is described by Marquiz and Nau on pp. 4387 ff.

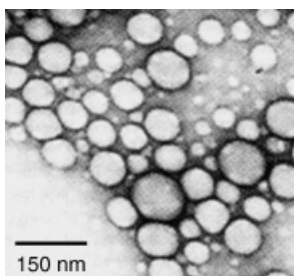


REVIEW

Contents

Aqueous, nanodispersed formulations of organic active compounds and effect materials (see electron micrograph) allow a dramatic increase in solubility, an improvement in biological absorption, and the modification of physical properties. The current state of knowledge of the basics of particle formation from homogeneous solution, the influence of the solvent and polymer additives on the morphology, and the supramolecular structure of the nanoparticles, is illustrated with the carotenoids, an industrially interesting class of compounds.

Angew. Chem. **2001**, *113*, 4460–4492

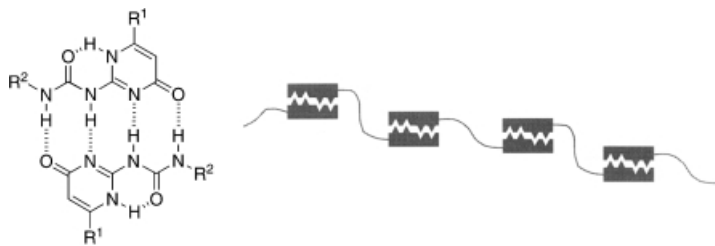


D. Horn, J. Rieger* 4330–4361

Organic Nanoparticles in the Aqueous Phase—Theory, Experiment, and Use

Keywords: carotenoids •
disperse systems • nanoparticles •
nanostructures • phase transformations

Four linearly arranged hydrogen bonds result in very efficient self-associating systems (left in the picture). Such quadruple hydrogen-bonding motifs offer the opportunity to obtain supramolecular polymers through the self-association of self-complementary monomers (shown schematically on the right). As the formation of noncovalent interactions is reversible and their strength depends on the external conditions, it is possible to influence the macroscopic properties of such polymers through altering the environment.



Angew. Chem. **2001**, *113*, 4493–4499

C. Schmuck,* W. Wienand 4363–4369

Self-Complementary Quadruple Hydrogen-Bonding Motifs as a Functional Principle: From Dimeric Supramolecules to Supramolecular Polymers

Keywords: dimerizations • heterocycles • hydrogen bonds • molecular recognition • polymers • supramolecular chemistry

ESSAY

Spatial and temporal resolution with, until recently, an unimaginable precision—about 0.01 Å and 10 fs, respectively—are today possible thanks to femtochemistry. However, this atomic-scale resolution raises fundamental questions from quantum mechanics: the Uncertainty Paradox. How is it that this is not an obstacle, and what are the future directions? are the themes of this Essay.

Angew. Chem. **2001**, *113*, 4501–4506

A. H. Zewail* 4371–4375

Chemistry at the Uncertainty Limit

Keywords: coherence • femtobiology • femtochemistry • spectroscopic methods • ultrafast electron diffraction

VIPs

The following communications are “Very Important Papers” in the opinion of two referees. They will be published shortly (those marked with a diamond will be published in the next issue). Short summaries of these articles can be found on the *Angewandte Chemie* homepage at the address <http://www.angewandte.com>

Design and Synthesis of a Peptide that Binds Specific DNA Sequences through Simultaneous Interaction in the Major and in the Minor Groove

Influence of Structural and Rotational Isomerism on the Triplet Blinking of Individual Dendrimer Molecules

Cesiumauride Ammonia (1/1: CsAu · NH₃)—A Crystalline Analogue of Alkali Metals Dissolved in Ammonia?

Enantiopure Double-Helical Acetylenic Cyclophanes

Supramolecular Cluster Catalysis: A Case Study of Benzene Hydrogenation Catalyzed by a Cationic Triruthenium Cluster under Biphasic Conditions

Syntheses and Crystal Structures of the First Disulfur and Diselenium Complexes of Platinum

Gold-Xenon Complexes

M. E. Vázquez, A. M. Caamaño,* ♦
J. Martínez-Costas, L. Castedo,
J. L. Mascareñas*

T. Vosch, J. Hofkens,* M. Cotlet, ♦
F. Köhn, H. Fujiwara,
R. Gronheid, K. Van Der Biest,
T. Weil, A. S. Herrmann,
K. Müllen, S. Mukamel,
M. Van der Auweraer,
F. C. De Schryver*

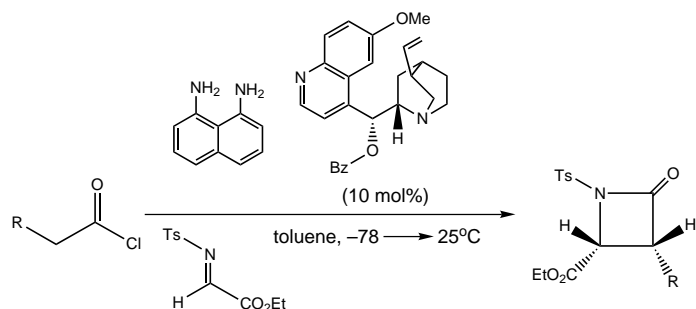
A.-V. Mudring, M. Jansen,*
J. Daniels, S. Krämer,
M. Mehring, J. P. Ramalho,
A. H. Romero, M. Parrinello
D.-L. An, T. Nakano, A. Orita,
J. Otera*

G. Süss-Fink,* M. Faure,
T. R. Ward

K. Nagata, N. Takeda,
N. Tokitoh*

S. Seidel, T. Drews, K. Seppelt*

Two direct catalytic asymmetric syntheses of β -lactams in good yields and high enantio- and diastereoselectivity (up to 96% *ee* and 99:1 d.r.) are described (see reaction scheme for an example). In addition, recent catalytic enantioselective constructions of β -amino acid derivatives en route to enantiomerically pure β -lactams are highlighted.



Angew. Chem. **2001**, *113*, 4507–4509

P. A. Magriotis* 4377–4379

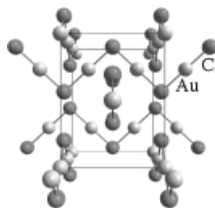
Recent Progress in the Enantioselective Synthesis of β -Lactams: Development of the First Catalytic Approaches

Keywords: amino acids • asymmetric catalysis • lactams • Lewis acids • Staudinger reaction

COMMUNICATIONS

Relativistic effects change the symmetry of the solid-state gold halides from a cubic to a chainlike AuX arrangement ($\text{X} = \text{F}, \text{Cl}, \text{Br}, \text{I}$; see structure of AuCl) with short $\text{Au}-\text{Au}$ internuclear distances. The main reason for the relativistic destabilization of the cubic and relativistic stabilization of the chainlike structures is a decrease in ionicity and an increase in covalency in the $\text{Au}-\text{X}$ interactions.

Angew. Chem. **2001**, *113*, 4511–4515



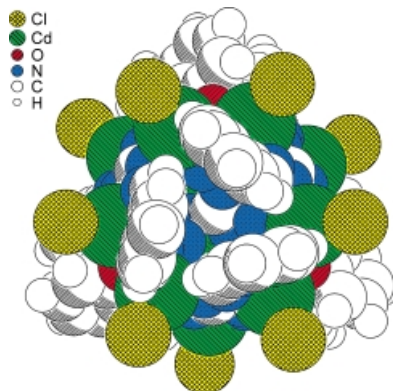
T. Söhnel, H. Hermann,
P. Schwerdtfeger* 4382–4385

Towards the Understanding of Solid-State Structures: From Cubic to Chainlike Arrangements in Group 11 Halides

Keywords: ab initio calculations • density functional calculations • gold • relativistic effects • solid-state structures

A sealed off capsule of composition $[\text{M}_{12}(\text{ligand})_4]$ containing a trapped Et_4N^+ ion has the topology of the tetrahedron in which the four nodes are provided by guanidine-based ligands and the six node-to-node connections are provided by pairs of metal centers (see picture).

Angew. Chem. **2001**, *113*, 4519–4520

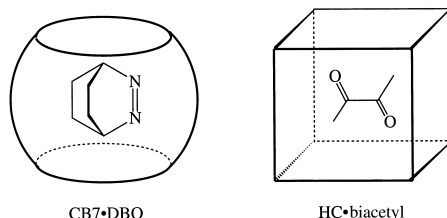


I. M. Müller, R. Robson,*
F. Separovic 4385–4386

A Metallosupramolecular Capsule with the Topology of the Tetrahedron, 3^3 , Assembled from Four Guanidine-Based Ligands and Twelve Cadmium Centers

Keywords: cage compounds • coordination chemistry • guanidine • nanostructures • supramolecular chemistry

A polarizability close to the gas phase is measured inside the cavity of the molecular container cucurbit[7]uril (CB7) by employing 2,3-diazabicyclo[2.2.2]oct-2-ene (DBO) as a solvatochromic guest (CB7·DBO). Conversely, the previously studied photophysical properties of biacetyl as a guest in a hemicarcerand (HC·biacetyl) indicate an exceptionally high polarizability inside this host cavity. These conclusions can be drawn from the solvatochromism of DBO and biacetyl in different solvents and the gas phase, which reveals correlations with the bulk polarizability. The oscillator strength, that is, the integrated absorption intensity, of the novel probes is not sensitive to the solvent polarity, but responds strongly to the solvent polarizability.



C. Marquez, W. M. Nau* ... 4387–4390

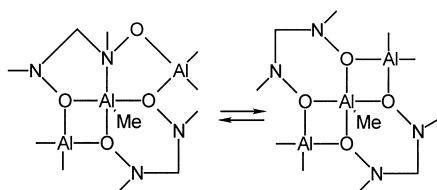
Polarizabilities Inside Molecular Containers

Keywords: cucurbituril • hemicarcerands • host–guest systems • solvatochromism • solvent effects

Angew. Chem. 2001, 113, 4515–4518

Four-, five-, and six-membered rings

surround a central five-coordinate aluminum atom in (AlMe)₂[(ONMe)₂CH₂]₂ in the solid state, but in solution all eight donor atoms are at some stage involved in bonding to this five-coordinate aluminum center (see scheme). This Al compound is formed from (HONMe)₂CH₂ and AlMe₃, whereas the reaction with GaMe₃ leads to the heteronorbomane (Me₂GaONMe)₂CH₂.



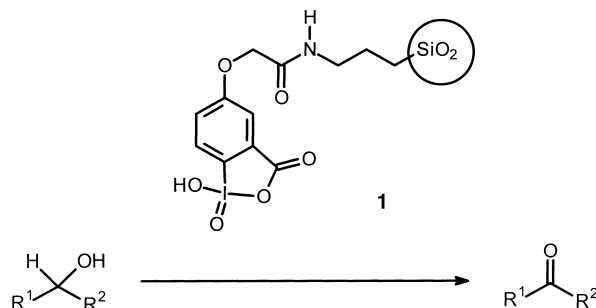
C. Lustig, N. W. Mitzel* ... 4390–4392

The Highly Flexible Bis(hydroxylamine) Ligand [ON(Me)₂CH₂]₂²⁻ and Its Different Behavior in the Chemistry of Aluminum and Gallium

Keywords: aluminum • gallium • molecular dynamics • N,O ligands

Angew. Chem. 2001, 113, 4521–4524

Primary and secondary alcohols are oxidized smoothly under mild conditions and in high yields to the corresponding aldehydes and ketones by **1** (see scheme), the first polymer-supported IBX.



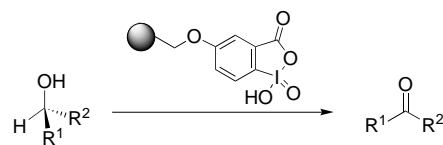
M. Mülbauer, A. Giannis* 4393–4394

The Synthesis and Oxidative Properties of Polymer-Supported IBX

Keywords: hypervalent compounds • iodine reagents • oxidation • solid-phase synthesis • synthetic methods

Angew. Chem. 2001, 113, 4530–4532

The oxidation of various alcohols and cyclization of an olefinic carbamate succeeds with the first polymer-supported iodine(v) reagent (see scheme). The novel oxidizing polymer oxidizes sensitive and complex alcohols, including protected amino alcohols, efficiently in good to excellent yields. In addition, the α,β -dehydration of a ketone is demonstrated.



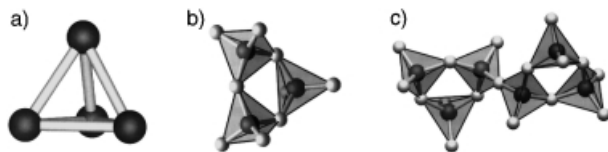
G. Sorg, A. Mengel, G. Jung, J. Rademann* ... 4395–4397

Oxidizing Polymers: A Polymer-Supported, Recyclable Hypervalent Iodine(v) Reagent for the Efficient Conversion of Alcohols, Carbonyl Compounds, and Unsaturated Carbamates in Solution

Keywords: hypervalent compounds • iodine reagents • oxidation • solid-phase synthesis • synthetic methods

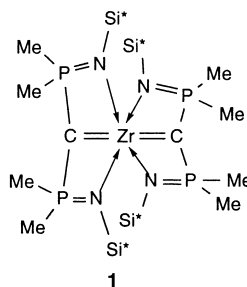
Angew. Chem. 2001, 113, 4532–4535

The previously unknown silicate ion $[\text{Si}_6\text{O}_{17}]^{10-}$ (c) and mixed-valent silicon centers that differ by five oxidation states are present in the tetrelide(−1)–tetrelate(+4) compound $\text{Cs}_{10}[\text{Si}_4][\text{Si}_3\text{O}_9]$ (anions a and b) and $\text{Rb}_{14}[\text{E}_4][\text{Si}_6\text{O}_{17}]$ (E = Si and Ge; anions a and c). The structures of this new class of compounds can be described by chemical twinning of the silicate and Zintl phases $\text{A}_4[\text{E}^{\text{IV}}]$.



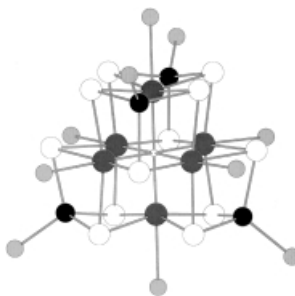
Angew. Chem. **2001**, *113*, 4527–4529

Two carbene ligands bound to zirconium: Complex **1** was synthesized under mild conditions by reaction of $\text{CH}_2(\text{Me}_2\text{P}=\text{NSiMe}_3)_2$ with $[\text{Zr}(\text{CH}_2\text{C}_6\text{H}_5)_4]$ in a 2:1 ratio. The resulting complex **1** is the first biscarbene complex of a Group 4 metal. $\text{Si}^* = \text{SiMe}_3$.



Angew. Chem. **2001**, *113*, 4535–4537

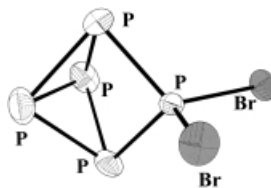
Silylated chalcogenides $(\text{Me}_3\text{Si})_2\text{E}$ (E = S, Se, Te) grant access to novel Nb–Cu chalcogenido clusters with as yet unknown molecular structures. Dimeric Nb–Cu selenido clusters $[\text{Cu}_4\text{Nb}_6\text{Se}_{12}\text{O}(\text{PMe}_3)_{10}][\text{Cu}_4\text{Nb}_6\text{Se}_4\text{Cl}_2(\text{PMe}_3)_4]$ (the structure of the cation is depicted; Cu: black, Nb: dark gray, P: light gray, Se: white O: small white) and $[\text{Cu}_4\text{Nb}_2\text{Se}_6(\text{PMe}_3)_8]$ were isolated from reactions of $(\text{Me}_3\text{Si})_2\text{Se}$ with Nb–Cu–Se units that were formed in situ. Reactions of CuCl and NbCl₅ towards $(\text{Me}_3\text{Si})_2\text{S}$ or $(\text{Me}_3\text{Si})_2\text{Te}$ produce the compounds $(\text{NEt}_4)[\text{Cu}_6\text{Nb}_2\text{S}_6\text{Cl}_5(\text{PET}_3)_6]$ and $[\text{Cu}_6\text{NbTe}_3(\text{Te}_2)_2(\text{PET}_3)_6][\text{CuCl}_2]$, respectively.



Angew. Chem. **2001**, *113*, 4537–4541

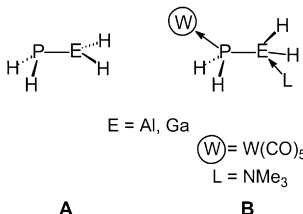


Insertion of the intermediately formed carbene-analogous PX_2^+ ion (X = Br, I) into one of the P–P bonds of the P_4 tetrahedron led to the P_5X_2^+ ion (see structure of the Br derivative)—the first example of the previously unknown class of phosphorus-rich binary P–X cations.



Angew. Chem. **2001**, *113*, 4544–4547

Neither synthesis nor detection in matrix isolation experiments has been accomplished for the parent compounds of phosphanylalanes and -gallanes of type **A**. H_2 elimination reactions between $[(\text{CO})_5\text{WPH}_3]$ and H_3ENMe_3 (E = Al, Ga) have enabled the first synthesis of Lewis acid/base stabilized complexes of the type **B**. Comprehensive density functional theory (DFT) calculations on the aluminum systems verify the high stability of the complexes of type **B**.



Angew. Chem. **2001**, *113*, 4541–4544

S. Hoffmann, T. F. Fässler,* C. Hoch,
C. Röhr* 4398–4400

Alkali Metal Tetrelide–Tetrelates:
“Double Salts” With $[\text{E}_4]^{4-}$ Zintl Anions
(E = Si, Ge) and the First Dimeric
Cyclotrisilicate Ions $[\text{Si}_6\text{O}_{17}]^{10-}$

Keywords: germanides • silicates •
silicides • Zintl anions • Zintl phases

K. Aparna, R. P. Kamalesh Babu,
R. McDonald, R. G. Cavell* 4400–4402

The First Biscarbene Complex of a
Group 4 Metal: $[\text{Zr}\{\text{C}(\text{Me}_2\text{P}=\text{NSiMe}_3)_2\}_2]$

Keywords: carbene ligands • coordination
chemistry • N,P ligands • zirconium

A. Lorenz, D. Fenske* 4402–4406

Syntheses and Structures of Niobium
Copper Chalcogenido Clusters:
 $[\text{Cu}_4\text{Nb}_6\text{Se}_{12}\text{O}(\text{PMe}_3)_{10}]$ –
 $[\text{Cu}_4\text{NbSe}_4\text{Cl}_2(\text{PMe}_3)_4] \cdot 1.5 \text{ DMF}$,
 $[\text{Cu}_4\text{Nb}_2\text{Se}_6(\text{PMe}_3)_8]$,
 $(\text{NEt}_4)[\text{Cu}_6\text{Nb}_2\text{S}_6\text{Cl}_5(\text{PET}_3)_6]$, and
 $[\text{Cu}_6\text{NbTe}_3(\text{Te}_2)_2(\text{PET}_3)_6][\text{CuCl}_2]$

Keywords: chalcogens • clusters •
copper • niobium

I. Krossing,* I. Raabe 4406–4409

P_5X_2^+ (X = Br, I), a Phosphorus-Rich
Binary P–X Cation with a C_{2v} -Symmetric
 P_5 Cage

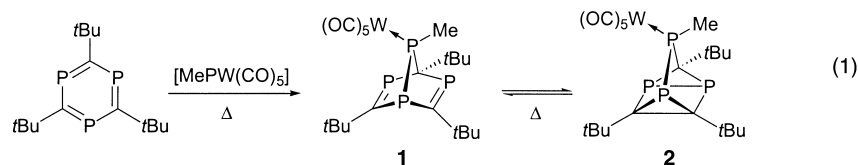
Keywords: ab initio calculations • cations •
halogens • insertion • phosphorus

U. Vogel, A. Y. Timoshkin,
M. Scheer* 4409–4412

Lewis Acid/Base Stabilized
Phosphanylalane and -gallane

Keywords: aluminum • density functional
calculations • gallium • Lewis acids •
phosphorus

Phosphorus changes stability: Investigation of the phosphorus polycycles **1** and **2**, prepared according to Equation (1), show that the relative stability of the norbornadiene and quadricyclane frameworks is inverted when four of the framework carbon atoms are replaced by phosphorus atoms. These organophosphorus compounds can be isolated at room temperature but are in equilibrium at elevated temperatures. The experimental findings are in agreement with the results of ab initio MO theory calculations.




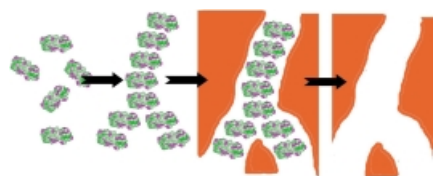
Angew. Chem. **2001**, *113*, 4524–4527

M. J. M. Vlaar, A. W. Ehlers, M. Schakel,
S. B. Clendenning, J. F. Nixon,
M. Lutz, A. L. Spek,
K. Lammertsma* 4412–4415

Norbornadiene–Quadricyclane Valence
Isomerism for a Tetraphosphorus
Derivative

Keywords: phosphinidene complexes •
phosphorus heterocycles • polycycles •
valence isomerism

 **Self-organization in aqueous media** studied indirectly: The aqueous phase is solidified by a silica sol–gel process, and the supramolecular aggregate is 1:1 cast into a solid silica matrix. For the model-system cyclodextrins it was shown that the cyclodextrin molecules self-assemble into “wormlike” aggregates in the porous silica (see scheme). By using this template, porous materials were obtained with promising properties such as a uniform pore system and smooth walls.



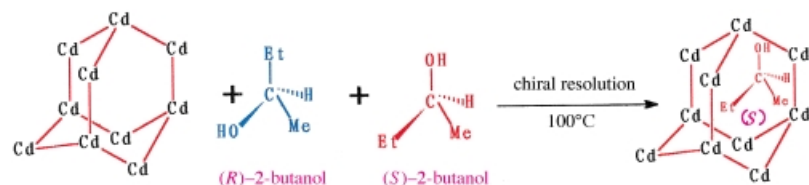
Angew. Chem. **2001**, *113*, 4549–4553

S. Polarz,* B. Smarsly, L. Bronstein,
M. Antonietti 4417–4421

From Cyclodextrin Assemblies to Porous
Materials by Silica Templating

Keywords: cyclodextrins • porous
materials • self-assembly

Selective inclusion of (*S*)-2-butanol and (*S*)-2-methyl-1-butanol from their racemic mixtures in 98.2 and 98.4% *ee*, respectively, is obtained with the robust 3D enantiopure hybrid organic–inorganic zeolite analogue [Cd(QA)₂] (see scheme), which is formed by self-assembly of chiral quinine (HQA) with Cd(OH)₂.




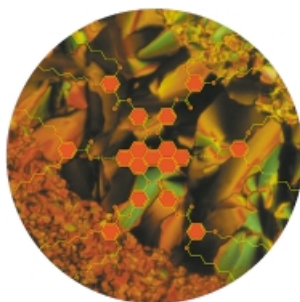
Angew. Chem. **2001**, *113*, 4554–4557

R.-G. Xiong,* X.-Z. You,
B. F. Abrahams, Z. Xue,
C.-M. Che 4422–4425

Enantioseparation of Racemic Organic
Molecules by a Zeolite Analogue

Keywords: cadmium • crystal
engineering • enantioseparation •
N ligands • zeolite analogues

 **Fluorescent liquid crystals:** Hydrogen bonding of benzoic acids to azaaromatic receptor groups of diazadibenzoperylene fluorophores induces columnar liquid crystalline mesophases which are highly fluorescent. The structure of a mesogenic supermolecule generated in this way is shown on a background of a polarizing micrograph of the resulting liquid crystalline phase.



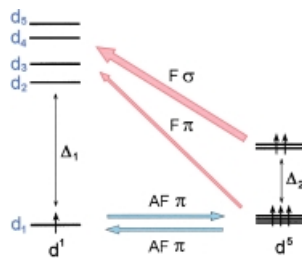
Angew. Chem. **2001**, *113*, 4557–4560

A. Sautter, C. Thalacker,
F. Würthner* 4425–4428

Control of Liquid Crystallinity of
Diazadibenzoperylene Dyes by Covalent
and Hydrogen-Bonded Attachment of
Mesogens

Keywords: fluorescence • hydrogen
bonds • liquid crystals •
perylene dyes • supramolecular chemistry

Explaining the magnetism in cyanide-based magnets: The origin of ferromagnetism (F) in the recently synthesized heteronuclear cyanide-bridged clusters and three-dimensional (3D) networks containing octacyanomethylates is elucidated. The main factor is the orthogonality of the “magnetic orbitals” of the octamethylates to the σ orbitals of all the bridging cyanides, which strongly reduces the antiferromagnetic (AF) contribution to the magnetism of these compounds. The kinetic contribution to the superexchange is shown schematically, the arrows show the direction of the electron transfer.



Angew. Chem. **2001**, *113*, 4561–4565

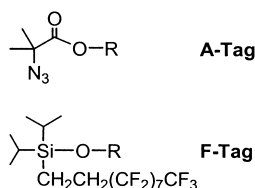
L. F. Chibotaru,* V. S. Mironov,
A. Ceulemans 4429–4433

Origin of Ferromagnetism in Cyano-
Bridged Compounds Containing d^1
Octacyanomethylates

Keywords: cyanides • magnetic
properties • manganese • metal–metal
interactions • molybdenum



React or get capped and tagged! Two capping reagents, designated A-Tag and F-Tag, mark unconverted oligosaccharides during automated synthesis for simple separation from the desired products. A-Tagged molecules are removed by an isocyanate scavenger resin after reduction to the amine, and those with an F-tag by filtration through fluorosilica gel. R = oligosaccharide.



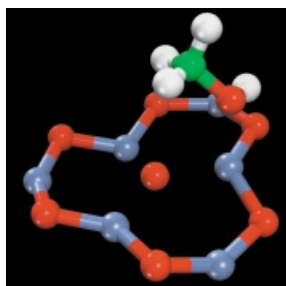
Angew. Chem. **2001**, *113*, 4565–4569

E. R. Palmacci, M. C. Hewitt,
P. H. Seeberger* 4433–4437

“Cap-Tag”—Novel Methods for the
Rapid Purification of Oligosaccharides
Prepared by Automated Solid-Phase
Synthesis

Keywords: oligosaccharides • solid-phase
synthesis • synthetic methods

The structures and energetics of the key intermediates in the catalytic conversion of CO_2 into methanol (shown in the figure) are investigated. The polarity of the catalytically relevant (000 $\bar{1}$) surface of ZnO gives rise to vacant oxygen sites, which by trapping electrons can promote the reaction. The solid-state embedding method developed is particularly well-suited to studying chemical processes on such localized active sites.



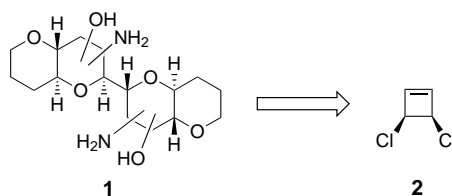
Angew. Chem. **2001**, *113*, 4569–4572

S. A. French,* A. A. Sokol, S. T. Bromley,
C. R. A. Catlow, S. C. Rogers, F. King,
P. Sherwood 4437–4440

From CO_2 to Methanol by Hybrid
QM/MM Embedding

Keywords: chemisorption • density
functional calculations • heterogeneous
catalysis • surface chemistry • zinc oxide

An efficient synthesis of cyclic polyether structures (e.g. **1**), which are commonly found in natural products, can be realized from *cis*-3,4-dichlorocyclobutadiene (**2**). The versatility of synthon **2** and a mechanistic rationale for the regio- and stereospecificity of the reactions is discussed.



Angew. Chem. **2001**, *113*, 4573–4577

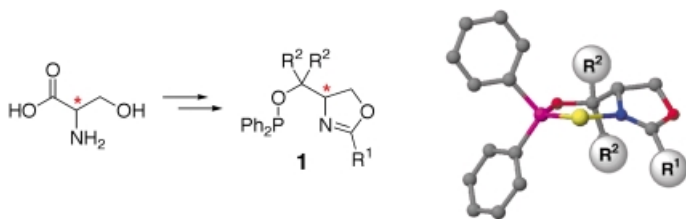
K. C. Nicolaou,* J. A. Vega,
G. Vassilikogiannakis 4441–4445

cis-3,4-Dichlorocyclobutene as a Versatile
Synthon in Organic Synthesis. Rapid
Entry into Complex Polycyclic Systems
with Remarkably Stereospecific
Reactions

Keywords: asymmetric synthesis •
cycloalkenes • metathesis • natural
products • polycyclic ethers



Both enantiomers are readily prepared of phosphinite–oxazoline ligands **1** from the D and L enantiomers of serine (see Scheme). Iridium complexes derived from these ligands (the structure of one complex is shown) are excellent catalysts for the enantioselective hydrogenation of unfunctionalized alkenes. R¹ = ferrocenyl, aryl; R² = alkyl, benzyl.



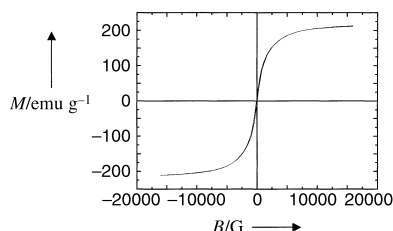
Angew. Chem. **2001**, *113*, 4577–4579

J. Blankenstein, A. Pfaltz* 4445–4447

A New Class of Modular Phosphinite–Oxazoline Ligands: Ir-Catalyzed Enantioselective Hydrogenation of Alkenes

Keywords: asymmetric catalysis • hydrogenation • iridium • ligand design • N,P ligands

A coating of iron carbide and carbon confers air-stability on the nanocrystalline iron particles that were prepared by sonolysis of [Fe(CO)₅] in diphenylmethane followed by annealing of the as-prepared material. The saturation magnetization of this material (222 emu g^{−1}, see picture) is almost as high as that of bulk bcc iron.



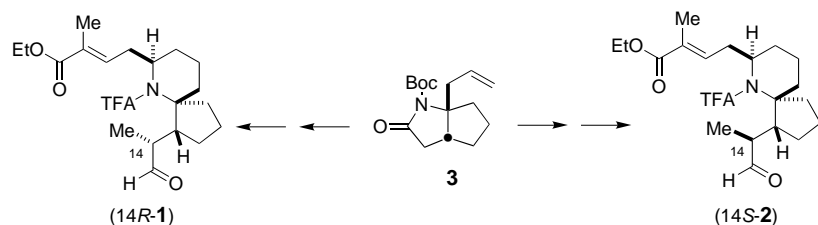
Angew. Chem. **2001**, *113*, 4579–4581

S. I. Nikitenko, Yu. Koltypin, O. Palchik, I. Felner, X. N. Xu, A. Gedanken* 4447–4449

Synthesis of Highly Magnetic, Air-Stable Iron–Iron Carbide Nanocrystalline Particles by Using Power Ultrasound

Keywords: carbides • iron • magnetic properties • nanostructures • sonochemistry

Important intermediates: in an effort to synthesize and determine the stereochemistry of pinnaic acid, C14-epimeric aldehydes **1** and **2** were generated from Meyers' lactam **3**. A key step in the parallel syntheses is a highly stereoselective vinylogous Michael cyclization; Boc = *tert*-butoxy carbonyl, TFA = trifluoroacetic acid.



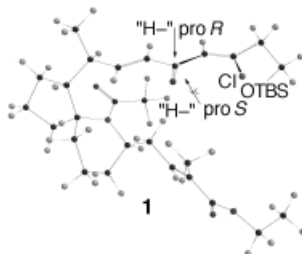
Angew. Chem. **2001**, *113*, 4582–4584

M. W. Carson, G. Kim, M. F. Hentemann, D. Trauner, S. J. Danishefsky* 4450–4452

Concise Stereoselective Routes to Advanced Intermediates Related to Natural and Unnatural Pinnaic Acid

Keywords: alkaloids • asymmetric synthesis • natural products • total synthesis

Build 'em up and knock 'em down: natural pinnaic acid and three of its stereoisomers were synthesized from the aldehydes described in the preceding communication. A key step in the synthesis of natural pinnaic acid was a highly stereoselective reduction of ketone **1**. The stereochemistry was determined by means of degradation studies of the synthetic material; TBS = *tert*-butyldimethylsilyl.



Angew. Chem. **2001**, *113*, 4585–4588

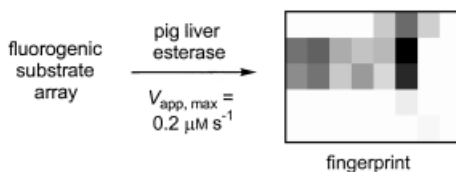
M. W. Carson, G. Kim, S. J. Danishefsky* 4453–4456

Total Synthesis and Proof of Stereochemistry of Natural and Unnatural Pinnaic Acids: A Remarkable Long-Range Stereochemical Effect in the Reduction of 17-Oxo Precursors of the Pinnaic Acids

Keywords: asymmetric synthesis • degradation • natural products • structure elucidation • total synthesis

Differentiation between different enzymes within one class is possible

by plotting the relative reaction rates of an enzyme with a series of chromogenic or fluorogenic enzyme substrates as an array of gray-scale squares (see scheme). The characteristic enzyme fingerprints obtained for hydrolytic enzymes such as lipases, esterases, amidases, and epoxide hydrolases are reproducible and enzyme specific. Such fingerprints may be used in quality controls, batch identification, and as screening tools in enzyme discovery programs.




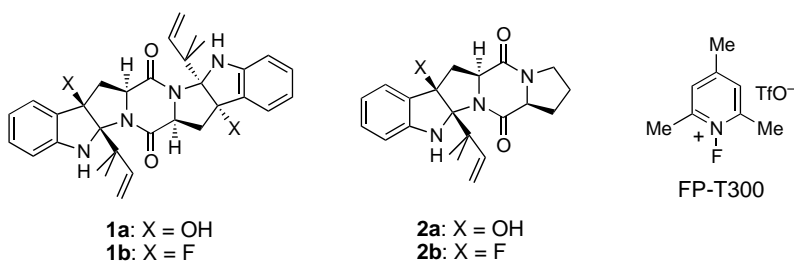
Angew. Chem. **2001**, *113*, 4589–4592

D. Wahler, F. Badalassi, P. Crotti,
J.-L. Reymond* 4457–4460

Enzyme Fingerprints by Fluorogenic and Chromogenic Substrate Arrays

Keywords: enzyme assays • enzyme catalysis • high-throughput screening • substrate arrays

 **Fluoro-isosteres of natural products** containing hexahydropyrazino[1',2'-1,5]pyrrolo[2,3-*b*]indole-1,4-dione moieties are readily prepared by FP-T300-mediated fluorination–cyclization of cyclo-Trp-AAs (Trp = tryptophan, AA = amino acid). Isosteres **1b** and **2b** of gypsetin (**1a**) and brevianamide E (**2a**), respectively, were thus synthesized.




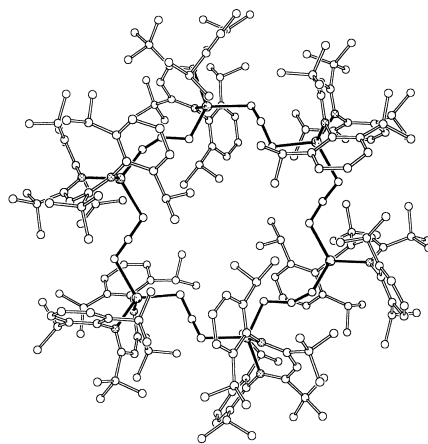
Angew. Chem. **2001**, *113*, 4593–4595

N. Shibata,* T. Tarui, Y. Doi,
K. L. Kirk 4461–4463

Synthesis of Fluorogypsetin and Fluorobrevianamide E by a Novel Fluorination–Cyclization of cyclo-L-Trp-L-AAs

Keywords: cyclization • diastereoselectivity • fluorine • natural products • total synthesis

 **The cyclic hexanuclear species** $[\{HC[C(tBu)NAr']_2Mg(C_3H_5)\}_6]$ (see structure) in which the allyl group exhibits $\mu\text{-}\eta^1\text{:}\eta^1$ bonding is formed on thermal treatment of $[HC[C(tBu)NAr']_2Mg(C_3H_5)(thf)]$ under vacuum. Ar' = 2,6-diisopropylphenyl.



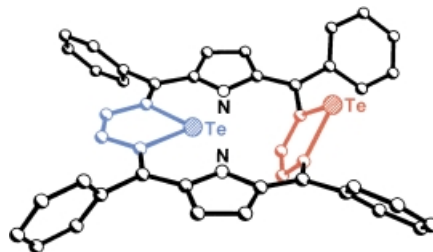
Angew. Chem. **2001**, *113*, 4595–4598

P. J. Bailey,* S. T. Liddle,*
C. A. Morrison, S. Parsons 4463–4466

The First Alkaline Earth Metal Complex Containing a $\mu\text{-}\eta^1\text{:}\eta^1$ Allyl Ligand: Structure of $[\{HC[C(tBu)NAr']_2Mg(C_3H_5)\}_6]$

Keywords: allyl ligands • alkaline earth metals • magnesium • N ligands • structure elucidation

The flexible partially inverted structure of an 18- π -electron porphyrin-(1.1.1.1)-like framework is found for 21,23-ditelluraporphyrin (see structure). The dihedral angle between the plane of *meso*-carbon atoms and the inverted tellurophene plane in the solid state is $123.0(2)^\circ$, while in solution the porphyrin molecule interchanges between two energetically identical flipped forms.



Angew. Chem. **2001**, *113*, 4598–4601

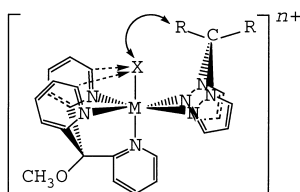
E. Pacholska, L. Latos-Grażyński,*
Z. Ciunik 4466–4469

An Unorthodox Conformation of [18]porphyrin-(1.1.1.1) Heteroanalogue—21,23-Ditelluraporphyrin with a Flipped Tellurophene Ring

Keywords: heteroporphyrins • nonplanar porphyrins • porphyrinoids • tellurophenes



Stung into action: The largest rate constant to date for ligand substitution at an Ru^{II} center ($110 \text{ M}^{-1} \text{ s}^{-1}$) was observed as a result of a heteroscorpionate ligand effect (see picture; $\text{X} = \text{H}_2\text{O}$, $\text{R} \neq \text{pyrazole}$, $\text{M} = \text{Ru}$) for the substitution of H_2O by CH_3CN .



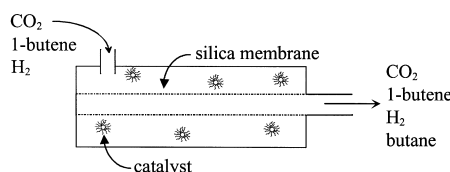
M. H. V. Huynh,* J. Smyth, M. Wetzler, B. Mort, P. K. Gong, L. M. Witham, D. L. Jameson, D. K. Geiger, J. M. Lasker, M. Charepoo, M. Gornikiewicz, J. M. Cintron, G. Imahori, R. R. Sanchez, A. C. Marschlok, L. M. Krajowski, D. G. Churchill, M. R. Churchill, K. J. Takeuchi * 4469–4473

Remarkable Rate Enhancement of Ligand Substitution Promoted by Geometrical Arrangement of Tridentate “Spectator” Ligands

Keywords: kinetics • ligand substitution • N ligands • ruthenium • scorpionates

Angew. Chem. **2001**, *113*, 4601–4605

Membrane separation technology is successfully applied for the immobilization of a homogeneous catalyst (a (1*H*,1*H*,2*H*,2*H*-perfluoroalkyl)-dimethylsilyl-substituted derivative of Wilkinson's catalyst) in a continuous process that uses supercritical carbon dioxide as solvent. The catalyst is separated from the products by a microporous silica membrane (see scheme).



L. J. P. van den Broeke,* E. L. V. Goetheer, A. W. Verkerk, E. de Wolf, B.-J. Deelman, G. van Koten, J. T. F. Keurentjes 4473–4474

Homogeneous Reactions in Supercritical Carbon Dioxide Using a Catalyst Immobilized by a Microporous Silica Membrane

Keywords: green chemistry • homogeneous catalysis • hydrogenation • membrane reactors • supercritical fluids

Angew. Chem. **2001**, *113*, 4605–4606

Nucleophilic addition to cycloalkenols has been achieved by catalytic electronic activation of the substrate. Catalyzed reversible conversion of the alcohol into a ketone causes electronic activation of the alkene, allowing nucleophilic addition to occur (see scheme).



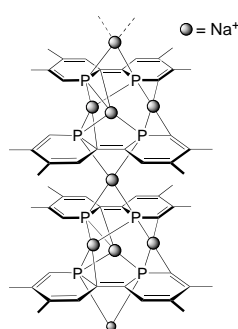
P. J. Black, W. Harris, J. M. J. Williams * 4475–4476

Catalytic Electronic Activation: Indirect Addition of Nucleophiles to an Allylic Alcohol

Keywords: aluminum • catalytic electronic activation • homogeneous catalysis • hydrogenation • Michael addition

Angew. Chem. **2001**, *113*, 4607–4608

A surprising polymeric structure (see picture) results from the two-electron reduction of a 2,2'-biphosphinine with sodium/naphthalene in dimethoxyethane. When reduction is carried out with lithium in the presence of (2.2.1) cryptand, the reduced ligand adopts a *trans* configuration in the solid state. DFT calculations clearly indicate a phosphaaallylic-type structure.



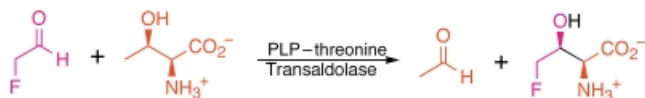
P. Rosa, N. Mézailles, L. Ricard, F. Mathey,* P. Le Floch* 4476–4479

The tmbp Dianion in the Contact Ion Pair $[(\text{tmbp})\text{Na}_2(\text{dme})_{1.5}]_n$ and in the Solvent-Separated Ion Pair $[\text{tmbp}][(\text{2.2.1})\text{Li}]_2$

Keywords: alkali metals • density functional calculations • phosphinines • phosphorus heterocycles • reduction

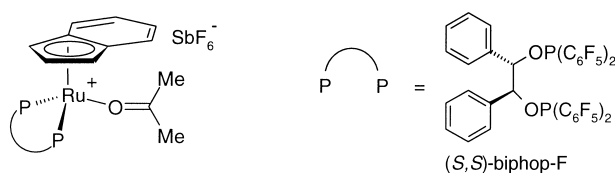
Angew. Chem. **2001**, *113*, 4608–4611

The final enzyme on the biosynthetic pathway to 4-fluorothreonine is identified in *Streptomyces cattleya*. The enzyme catalyzes a pyridoxal phosphate-dependent “transaldose” reaction between L-threonine and fluoroacetaldehyde (see scheme; PLP = pyridoxal 5'-phosphate). Unlike threonine aldolases, glycine is not a substrate for this new type of enzyme.



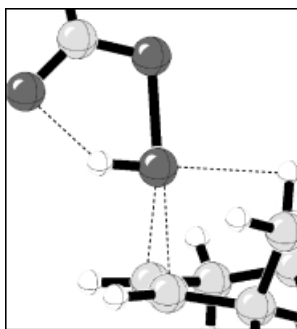
Angew. Chem. **2001**, *113*, 4611–4613

The indenyl roof over the chiral Lewis acid catalyst site of [(indenyl)Ru((*S,S*)-biphop-F)]⁺ (see picture) gives rise not only to high enantioselectivities in Diels–Alder reactions between enals and cyclopentadiene but also affects the *endo/exo* diastereoselectivity. The *exo* product is formed preferentially even with acrolein.



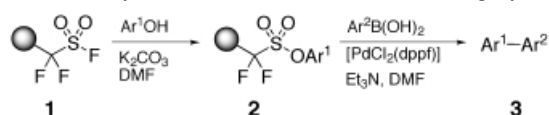
Angew. Chem. **2001**, *113*, 4613–4617

Peracids prefer to attack *syn* to an alkyl group as shown by the most stable transition state for the epoxidation of 3-methylcyclohexene (see section of transition state). Computational and experimental evidence explain the origin of this effect and how it might be exploited in synthesis.



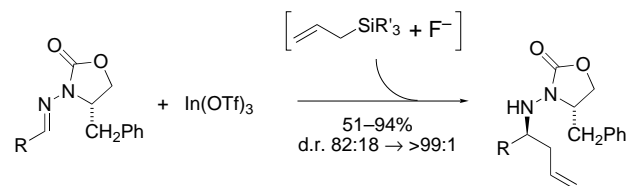
Angew. Chem. **2001**, *113*, 4617–4620

Three roles for the PFS fluoride resin 1: a linker, a protecting group, and an activating group for phenols. Immobilized “aryl triflates” **2** are generated upon treatment of **1** with phenols. Through a subsequent Suzuki cleavage/cross-coupling reaction an additional aryl group can be appended to the initial phenol to afford biaryls **3** in a “traceless” fashion in high yields.



Angew. Chem. **2001**, *113*, 4620–4623

A mild, convenient, and stereoselective addition of allylsilanes to enantiopure *N*-acylhydrazones occurs at room temperature upon complementary activation of both the allylsilane and the hydrazone (see scheme; OTf = trifluoromethanesulfonate). The reaction provides a new mode of acyclic stereocontrol for the asymmetric synthesis of homoallylic amines.



Angew. Chem. **2001**, *113*, 4623–4625

C. D. Murphy, D. O'Hagan,*
C. Schaffrath 4479–4481

Identification of a PLP-Dependent Threonine Transaldolase: A Novel Enzyme Involved in 4-Fluorothreonine Biosynthesis in *Streptomyces cattleya*

Keywords: biosynthesis • enzyme catalysis • fluorine • natural products • transaldolase

E. P. Kündig,* C. M. Saudan, V. Alezra,
F. Viton, G. Bernardinelli 4481–4485

[(Indenyl)Ru(biphop-F)]⁺: A Lewis Acid Catalyst That Controls both the Diene and the Dienophile Facial Selectivity in Diels–Alder Reactions

Keywords: asymmetric catalysis • cycloaddition • Lewis acids • P ligands • ruthenium

I. Washington, K. N. Houk * 4485–4488

CH···O Hydrogen Bonding Influences π -Facial Stereoselective Epoxidations

Keywords: ab initio calculations • diastereoselectivity • epoxidation • oxidation • peroxides

Y. Pan, B. Ruhland,
C. P. Holmes* 4488–4491

Use of a Perfluoroalkylsulfonyl (PFS) Linker in a “Traceless” Synthesis of Biaryls through Suzuki Cleavage

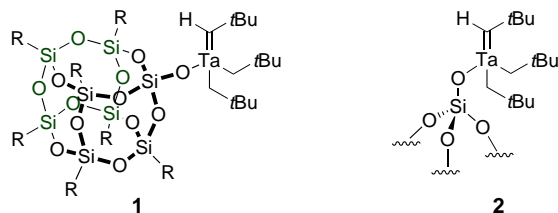
Keywords: biaryls • C–C coupling • combinatorial chemistry • solid-phase synthesis • synthetic methods

G. K. Friestad,* H. Ding ... 4491–4493

Asymmetric Allylsilane Additions to Enantiopure *N*-Acylhydrazones with Dual Activation by Fluoride and In(OTf)₃

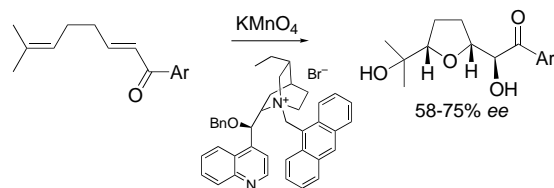
Keywords: allylation • amines • asymmetric synthesis • chiral auxiliaries • hydrazones

Feher cage analogues, such as **1**, provide easy access to models of surface structures such as **2**, and give a better understanding of surface reactions. In addition, surface complexes such as **2** can be fully characterized by high-resolution 1D and 2D solid-state NMR spectroscopy.



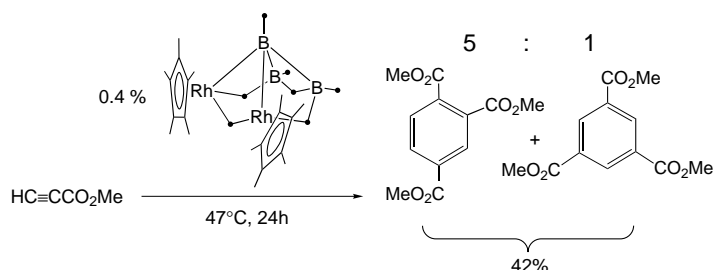
Angew. Chem. **2001**, *113*, 4625–4628

Up to four new stereocenters are created with control of the relative and absolute stereochemistry in a single step in the unusual phase-transfer-catalyzed oxidative cyclization of achiral dienes with permanganate (see scheme).



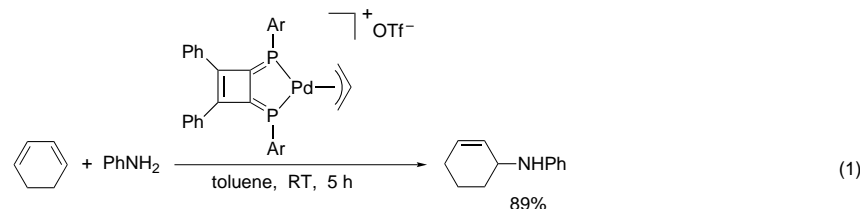
Angew. Chem. **2001**, *113*, 4628–4630

Catalysis with clusters: Transition metal characteristics control metallaborane reactivity as demonstrated by the reaction of a pair of isoelectronic and nearly isostructural metallaboranes with substituted alkynes. Novel catalytic chemistry of *nido*-[1,2-(Cp**Rh*)₂B₃H₇] and *nido*-[2,3-(Cp**Rh*)₂B₃H₇] (shown) with alkynes (see scheme) is observed with activities and selectivities that depend on catalyst structure and the alkyne substituents.



Angew. Chem. **2001**, *113*, 4630–4633

Room-temperature hydroamination of 1,3-dienes with aniline [Eq. (1)] is efficiently catalyzed by cationic η^3 -allyl palladium complexes, prepared by treating [$\{(\eta^3\text{-allyl})\text{PdCl}\}_2$] with 1,2-diaryl-3,4-bis[(2,4,6-tri-*tert*-butylphenyl)phosphinidene]cyclobutenes and AgOTf in CH₂Cl₂; Ar = 2,4,6-tri-*tert*-butylphenyl.



Angew. Chem. **2001**, *113*, 4633–4635

Supporting information on the WWW
(see article for access details).

M. Chabanas, E. A. Quadrelli, B. Fenet,
C. Copéret,* J. Thivolle-Cazat,
J.-M. Basset,* A. Lesage,
L. Emsley* 4493–4496

Molecular Insight Into Surface
Organometallic Chemistry Through the
Combined Use of 2D HETCOR Solid-
State NMR Spectroscopy and
Silsesquioxane Analogues

Keywords: NMR spectroscopy •
organometallic chemistry • silicates •
surface chemistry • tantalum

R. C. D. Brown,* J. F. Keily 4496–4498

Asymmetric Permanganate-Promoted
Oxidative Cyclization of 1,5-Dienes by
Using Chiral Phase-Transfer Catalysis

Keywords: asymmetric synthesis •
cyclization • dienes • diols • phase-
transfer catalysis

H. Yan, A. M. Beatty,
T. P. Fehlner* 4498–4501

Reactivity of Dimetallapentaboranes—
nido-[Cp*₂M₂B₃H₇]—with Alkynes:
Insertion to Form a Ruthenacarborane
(M = RuH) versus Catalytic
Cyclotrimerization to Form Arenes
(M = Rh)

Keywords: alkynes • boranes • cluster
compounds • homogeneous catalysis •
transition metals

T. Minami, H. Okamoto, S. Ikeda,
R. Tanaka, F. Ozawa,*
M. Yoshifuji 4501–4503

(η^3 -Allyl)palladium Complexes Bearing
Diphosphinidenecyclobutene Ligands:
Highly Active Catalysts for the
Hydroamination of 1,3-Dienes

Keywords: homogeneous catalysis •
hydroamination • nucleophilic addition •
palladium • P ligands

* Author to whom correspondence should be addressed



BOOKS

Dictionary of Gene Technology	Günther Kahl	<i>S. Brakmann</i> 4505
Carbohydrates	Robert V. Stick	<i>T. Ziegler</i> 4505
Green Chemical Syntheses and Processes	Paul T. Anastas, Lauren G. Heine, Tracy C. Williamson	<i>G. Kaupp</i> 4506
Computational Organometallic Chemistry	Thomas R. Cundari	<i>T. Strassner</i> 4508
DNA Arrays	Jang B. Rampal	<i>C. M. Niemeyer</i> 4510
Inorganic and Organometallic Polymers	Roland D. Archer	<i>D. Wöhrle</i> 4510
Fundamentals of Electroanalytical Chemistry	Paul M. S. Monk	<i>H. H. Girault</i> 4511
Kinetics of Homogeneous Multistep Reactions	F. G. Helfferich	<i>D. G. Blackmond</i> 4512
Heinrich Caro and the Creation of Modern Chemical Industry	Carsten Reinhardt, Anthony S. Travis	<i>H.-J. Quadbeck-Seeger, S. Becker</i> 4513



WEB SITES

http://webbook.nist.gov/chemistry	Thermochemistry Standards	<i>D. Schröder</i> 4515
---	------------------------------	-------------------------------

SERVICE

• VIPs	4312	• Keywords	4516
• <i>Angewandte's</i> Sister-Journals	4325–4327	• Authors	4517
• Sources	A137	• Preview	4518
• Vacancies	A139		

Don't forget all the Tables of Contents from 1998 onwards may be still found on the WWW under:
<http://www.angewandte.com>

Issue 22, 2001 was published online on November 16

CORRIGENDUM

In the second paragraph of the communication by **D. B. Grotjahn et al.** (*Angew. Chem. Int. Ed.* **2001**, 20, 3884–3887), previous work on complexes of electron-rich or chelating ligands with the CpRuCl fragment was reported (T. Suzuki, M. Tokunaga, Y. Wakatsuki, *Org. Lett.* **2001**, 3, 735–737). The best catalyst in this work was the complex [CpRuCl(Ph₂PCH₂PPh₂)] and not the complex [CpRuCl(Me₂PCH₂PMe₂)] given as an example. Thus, the first sentence of the following paragraph should be: “In contrast, here we report that electron-rich or chelating phosphanes are not needed.” The authors apologize for the error.